European Journal of Cancer 106 (2019) 160–170

Available online at www.sciencedirect.com

ScienceDirect

journal homepage: www.ejcancer.com

Original Research

Membrane human equilibrative nucleoside transporter 1 is associated with a high proliferation rate and worse survival in resected intrahepatic cholangiocarcinoma patients not receiving adjuvant treatments

S. Tavolari [a,b,1], M. Deserti [a,b,1], F. Vasuri [c], S. Curti [d], A. Palloni [a], A.D. Pinna [e], M. Cescon [e], G. Frega [a], S. De Lorenzo [a], M.A. Barbera [a], I. Garajova [a], L. Ricciardiello [d], D. Malvi [c], A. D'Errico-Grigioni [c], M.A. Pantaleo [a], G. Brandi [a,b,*,2]

[a] *Department of Experimental, Diagnostic and Specialty Medicine, S. Orsola-Malpighi University Hospital, Bologna, Italy*
[b] *Center for Applied Biomedical Research, S. Orsola-Malpighi University Hospital, Bologna, Italy*
[c] *"F. Addarii" Institute of Oncology and Transplantation Pathology, S. Orsola-Malpighi University Hospital, Bologna, Italy*
[d] *Department of Medical and Surgical Sciences, S. Orsola-Malpighi University Hospital, Bologna, Italy*
[e] *Division of Surgery and Transplantation, S. Orsola- Malpighi University Hospital, Bologna, Italy*

Received 31 July 2018; received in revised form 26 October 2018; accepted 1 November 2018
Available online 5 December 2018

KEYWORDS
Intrahepatic cholangiocarcinoma;
Human equilibrative nucleoside transporter 1;
Tissue biomarkers

Abstract Human equilibrative nucleoside transporter 1 (hENT-1) is a membrane nucleoside transporter mediating the intracellular uptake of nucleosides and their analogues. hENT-1 was recently reported to have a predictive role in intrahepatic cholangiocarcinoma (iCC) patients receiving adjuvant gemcitabine-based chemotherapy, but its biological and clinical significance in iCC remains unsettled. This study investigated the role of hENT-1 in regulating tumour growth and predicting the survival of 40 resected iCC patients not receiving adjuvant treatments. hENT-1 expression was found to be significantly higher in iCC than in the matched non-tumoural liver. Patients harbouring hENT-1 localised on the tumour cell membrane had a worse overall survival than membrane hENT-1–negative patients (median 21.2 months *vs* 30.3 months, $p = 0.031$), with an adjusted hazard ratio of 2.8 (95% confidence interval 1.01–7.76). Moreover, membrane hENT-1–positive patients had a higher percentage of Ki67-positive cells in tumour tissue than membrane hENT-1-negative patients (median 23% *vs* 5%, $p < 0.0001$). Functional analyses in iCC cell lines revealed that hENT-1 silencing inhibited

* *Corresponding author*: Department of Experimental, Diagnostic and Specialty Medicine, S. Orsola-Malpighi University Hospital, via Massarenti 9, 40138, Bologna, Italy. Fax: +39 051 2144037.
E-mail address: giovanni.brandi@unibo.it (G. Brandi).
[1] Contributed equally to this work. [2] on behalf of G.I.CO. (Gruppo Italiano COlangiocarcinoma).

https://doi.org/10.1016/j.ejca.2018.11.005

cell proliferation and induced apoptosis in HUH-28 cells expressing hENT-1 on the cell membrane, but not in SNU-1079 cells expressing the transporter only in the cytoplasm. Overall, these findings suggest that membrane hENT-1 is involved in iCC proliferation and associated with worse survival in resected iCC patients. Further prospective studies on larger cohorts are required to confirm these results and better define the potential prognostic role of membrane hENT-1 in this setting of patients.

1. Introduction

Intrahepatic cholangiocarcinoma (iCC) is a malignancy arising from the epithelial cells of the intrahepatic bile ducts and represents the second most common primary liver cancer after hepatocellular carcinoma [1]. Currently, the prognosis for iCC is discouraging, with the majority of patients not eligible for surgical resection (the only chance of long-term survival) and a five-year overall survival (OS) of approximately 5%–10% [2]. Unfortunately, the prognosis remains disappointing after curative-intent surgery, with a five-year survival rate ranging from 20% to 40% [3]. Although some clinicopathological variables (including tumour differentiation, staging, lymph node metastasis, nerve invasion, tumour size, resection margins and tumour location) have been suggested as prognostic factors in iCC patients after surgical resection [4], few data have been reported on putative prognostic tissue biomarkers in this setting of patients.

Human equilibrative nucleoside transporter 1 (hENT-1) is a membrane nucleoside transporter expressed in most human cells [5]. Besides mediating the intracellular uptake of nucleoside analogue drugs, hENT-1 regulates the physiological cellular uptake of purine and pyrimidine nucleosides, the precursors of nucleotide triphosphates (NTPs) that are essential for DNA and RNA synthesis [5]. We recently reported that proper hENT-1 localisation on the tumour cell membrane is associated with a longer disease-free survival in cholangiocarcinoma (CC) patients who have undergone more than four cycles of adjuvant gemcitabine-based chemotherapy [6].

The present study aimed to investigate the hypothesis that aberrant localisation of hENT-1 in tumour cells may also affect iCC tumour growth and patients' survival, due to impaired nucleoside uptake within tumour cells.

2. Materials and methods

2.1. Patients

Ninety-eight consecutive iCC patients underwent surgery with curative intent at S. Orsola-Malpighi University Hospital (Bologna, Italy) between January 2002 and December 2009. After radical resection (R0 or R1), patients meeting the following criteria were considered suitable for gemcitabine adjuvant chemotherapy: age $\geq$18 years, Eastern Cooperative Oncology Group Performance Status Scale (ECOG PS) $\leq$2, adequate white blood cell count, neutrophil count, platelet count, serum creatinine concentration and normal liver function values. Patients older than 77 years, with low ECOG PS (>2), impaired left ventricular ejection fraction or abnormal respiratory patterns or patients with white blood cell count <3500/Ml, platelet count <100,000/μL, renal dysfunction (creatinine concentration $\geq$1.5× normal) or hepatic dysfunction (bilirubin and aspartate aminotransferase levels more than twice the upper normal value) were considered unfit for adjuvant treatment [6,7]. Given the absence of any conclusive data on the efficacy of adjuvant chemotherapy after resection in CC, the decision on postoperative chemotherapy was left to the patient. Only iCC patients who did not receive adjuvant gemcitabine because they declined treatment were considered eligible for the present study, even if they met the criteria listed above. After surgery, patients were enrolled in a predefined follow-up program with visits every four months for the first two years and every six months thereafter. For patients who died, the survival time after surgery and cause of death were recorded.

Morphological classification of the tumours was based on the World Health Organisation criteria [8]. Tumours were graded as per the international tumour-node-metastasis system [9]. The study was carried out in accordance with the ethical guidelines of the 1975 Declaration of Helsinki (and subsequent modifications).

2.2. Tissue microarray and immunohistochemistry

Tissue microarray (TMA) was constructed from formalin-fixed, paraffin-embedded tissue samples from each iCC patient. To account for intratumor heterogeneity in this malignancy [10], three representative neoplastic cores for each case and two cores from the matched non-tumoural liver were assembled in the TMA block. Immunohistochemistry (IHC) for hENT-1 and Ki67 was performed on serial 3-μm-thick sections with anti–hENT-1 (GeneTex, Inc. San Antonio, TX, USA) and anti-Ki67 (clone 30-9; Ventana Medical

Systems, Tucson, AZ, USA) antibodies, respectively. IHC for hENT-1 was carried out with the Novolink Polymer Detection System (Leica Microsystems, Germany) as previously reported [6].

A tumour was considered positive for membrane hENT-1 localisation when at least two out of three TMA iCC cores showed membrane positivity. For Ki67 evaluation, IHC was automatically performed using a Benchmark Ultra immunostainer (Ventana/Roche) in accordance with the following protocol: (a) dewaxing; (b) antigen retrieval in cell conditioning 1 for 36 min at 95 °C; (c) incubation with primary antibody for 32 min at 37 °C and (d) development using the UltraView Alkaline Phosphatase Red detection kit and counterstaining in haematoxylin II. Ki67 was considered overexpressed when ≥10% stained nuclei were observed in each TMA core. For each patient, the overall Ki67 labelling index was obtained from the mean value of three TMA cores. IHC was evaluated by three dedicated pathologists blinded to each other and to clinical data and patient outcomes.

2.3. Cell lines

The human iCC cell lines SNU-1079 and HUH-28 were obtained from the Korean Cell Line Bank (Seoul, Korea). Cell lines were cultured in Roswell Park Memorial Institute's medium (Euroclone, Milan, Italy), supplemented with 10% (v/v) heat-inactivated foetal bovine serum (Euroclone), 2 mM L-glutamine, 100 U/ml penicillin and 100 μg/ml streptomycin (Sigma–Aldrich, St. Louis, MO, USA). Cells were grown at 37 °C in a humidified atmosphere of 95% air and 5% CO_2 and routinely passaged using 0.025% trypsin–ethylene diamine tetra-acetic acid (Euroclone).

2.4. hENT-1 siRNA transfection

For hENT-1 siRNA transfection, SNU-1079 (2×10^5) and HUH-28 (1×10^4) cells were seeded in a six-well plate in antibiotic-free medium. Transfection was performed with Lipofectamine (Invitrogen) in Opti-minimum essential medium (MEM) medium (Invitrogen) following the manufacturer's instructions. hENT-1 silencing was carried out by TriFECTa RNAi Kit (IDT, Coralville, USA) following the manufacturer's protocol. A scramble siRNA was used on each experiment as a negative control. RNA and proteins were extracted 48 and 72 h after siRNA transfection.

2.5. RNA isolation and quantitative reverse-transcriptase polymerase chain reaction

Total RNA was isolated from tissue samples and cell lines using the AllPrep DNA/RNA Mini Kit (Qiagen, Valencia, CA) as per the manufacturer's instructions. A total of 0.5 μg of RNA was reverse-transcribed using ImProm-II Reverse Transcriptase (Promega Corporation, Madison, USA) following the manufacturer's protocol. hENT-1 and glyceraldehyde 3-phosphate dehydrogenase (GAPDH) mRNA levels were analysed by quantitative reverse-transcriptase polymerase chain reaction using TaqMan Gene Expression Assays (Applied Biosystems, Carlsbad, CA, USA). Gene expression was expressed as ΔCt (Ct of the gene of interest normalised to Ct of GADPH). Fold change in mRNA expression was calculated based on the $2^{-\Delta\Delta Ct}$ method.

2.6. Immunocytochemistry

HuH-28 and SNU-1079 cells were seeded (2.5×10^4 cells/well) on a slide in a six-well plate and left to grow for 24 h. After a wash with PBS, cells were fixed with 4% paraformaldehyde for 5 min at room temperature. Cells were then washed with PBS, permeabilized with 0.5% Triton X-100 for 4 min, washed with PBS, incubated with PBS-BSA 3% for 30 min and subsequently with primary anti-hENT1 antibody (GeneTex, Inc. San Antonio, TX, USA), diluted 1:100 at 4 °C overnight. Following primary antibody incubation, cells were washed with phosphate-buffered solution (PBS) and incubated with secondary antibodies for 1 h at room temperature. Cells were then washed with PBS, distilled H_2O and finally developed in 3,3′-diaminobenzidine and counterstained with haematoxylin.

2.7. Nuclear morphological changes

Changes in nuclear morphology of SNU-1079 and HuH-28 cells transfected with hENT-1 siRNA were detected by the DNA-binding fluorochrome bis-benzimide stain (Hoechst 33,342; Sigma Chemical Co.). Briefly, SNU-1079 (2×10^5) and Huh-28 (1×10^4) cells were seeded in a six-well plate on a cover glass and transfected with hENT-1 siRNA as above described. At the end of incubation, 1 mg/ml Hoechst was added to each well for 30 min at 37 °C in the dark. Cells were finally washed twice with PBS and photographed under a fluorescence microscope (Nikon Eclipse; Florence, Italy).

2.8. Western blot analysis

Proteins were extracted from tumour tissues and matched normal livers with radioimmunoprecipitation assay (RIPA) Lysis and Extraction Buffer (G-Biosciences, St. Louis, MO, USA) supplemented with cOmplete Mini protease inhibitors (Roche, Mannheim, Germany) and phosphatase inhibitors (Roche). In Huh-28 and SNU-1079 cell lines, cytosolic and membrane protein fractions were extracted using the Compartmental Protein Extraction Kit (Millipore), as per the manufacturer's instructions. Equal amounts of protein extracts were then separated in 12% sodium dodecyl sulfate polyacrylamide *gel* electrophoresis (SDS-PAGE) and gels and transferred to polyvinylidene difluoride membranes by standard

methods. Membranes were immunoblotted with the following primary antibodies: anti–equilibrative nucleoside transporter (ENT-1) (Abcam), anti–caspase-3 (Cayman Chemical Company, Ann Arbor, MI, USA), anti–poly-(ADP-ribose)polymerase-1 (PARP-1) (Santa Cruz Biotechnology, Santa Cruz, CA, USA) and anti–β-actin (Cell Signalling, Danvers, MA, USA). Digital images of X-ray films were quantified by ChemiDoc XRS+ (Image Lab Software, Bio-Rad).

2.9. Cell viability assays

Methyltetrazolium (MTT) and crystal violet colorimetric assays were used to assess cell viability. For each type of experiment, HuH-28 and SNU-1079 cells (1×10^4 cells/well) were plated in a 24-well plate in triplicate and allowed to adhere for 24 h. Cells were then transfected with hENT-1 siRNA as above described; after transfection, they were grown for 24, 48 and 72 h. At the end of incubation, cells were processed as follows: (a) MTT was added to each well, and cells were incubated at 37 °C for 4 h. Formazan crystals were then dissolved in dimethyl sulfoxide (DMSO) and absorbance measured at 570 nm in a spectrophotometer (Thermofisher, USA); (b) cells were washed with PBS, fixed in 4% formaldehyde and stained with 1% crystal violet. Cells were washed twice with distilled H_2O and dried completely. Crystal violet was solubilised with 10% acetic acid for 15 min and absorbance was measured at 570 nm in a spectrophotometer (Thermofisher, USA).

2.10. Cell cycle analysis

Cell cycle analysis was performed by flow cytometry. For this purpose, Huh-28 and SNU-1079 cells were seeded in 25 cm^2 flasks at a density of 4×10^5 and transiently transfected with hENT-1 siRNA as previously described. After 72 h, cells were harvested by trypsinization, washed with PBS and incubated at 4 °C for 16 h in the DNA-staining solution (0.1% Triton X-100, 0.1% sodium citrate and 50 μg/ml propidium iodide). DNA content was finally analysed using the FACSAria cell sorter (Becton Dickinson, Franklin Lakes, NJ, USA).

2.11. Statistical analysis

Summary statistics of continuous variables were expressed as median (range) and compared using Mann–Whitney U test. Categorical variables were reported as numbers (percentages) and compared with Pearson's chi-squared test or Fisher's exact test, as appropriate. The main outcome measure was OS defined as the time from the date of iCC surgery to the date of death or the last follow-up. Data cut-off for OS analysis was December 31, 2016. Patients' survival curves were plotted using the Kaplan–Meier method, and differences between groups were compared by log-rank test.

The association between hENT-1 localisation in tumour cells and OS was characterised by hazard ratios (HRs) along with their 95% confidence intervals (CIs). The limited number of patients did not allow the inclusion of all covariates in multivariable Cox proportional hazards regression models. Due to problems of sparse data, we did not retain the full model (i.e., adjusted for all potential confounders), but we ran a reduced model using the backwards procedure where the selection of the covariates was based on the relative change-in-estimate approach [11]. In addition to the forced variables (i.e., age and gender), we finally included disease stage, histological grade and tumour size at surgery. Age was included as a categorical variable based on tertiles, whereas tumour size was entered in the model as a binary variable on the basis of the

Table 1
Baseline characteristics of the 40 iCC patients included in the study based on membrane hENT-1 localisation.

Characteristics	Total (n = 40)	Membrane hENT-1		p-value
		Negative (n = 27)	Positive (n = 13)	
Age at surgery (yr) median (range)	63.5 (34–77)	62 (34–77)	65 (46–76)	0.73[a]
Gender, n (%)				
female	21 (52.5)	16 (59.3)	5 (38.5)	0.22[b]
male	19 (47.5)	11 (40.7)	8 (61.5)	
Disease stage, n (%)				
I	6 (15.0)	4 (14.8)	2 (15.4)	0.99[c]
II	14 (35.0)	9 (33.4)	5 (38.4)	
III	10 (25.0)	7 (25.9)	3 (23.1)	
IV	5 (12.5)	4 (14.8)	1 (7.7)	
NA	5 (12.5)	3 (11.1)	2 (15.4)	
Size and extent (T), n (%)				
T1	3 (7.5)	1 (3.7)	2 (15.4)	0.35[c]
T2	24 (60.0)	18 (66.7)	6 (46.1)	
T3	11 (27.5)	7 (25.9)	4 (30.8)	
NA	2 (5.0)	1 (3.7)	1 (7.7)	
Regional lymph nodes (N), n (%)				
N0	21 (52.5)	15 (55.6)	6 (46.1)	0.90[c]
N1	12 (30.0)	8 (29.6)	4 (30.8)	
NA	7 (17.5)	4 (14.8)	3 (23.1)	
Distant metastases (M), n (%)				
M0	31 (77.5)	21 (77.8)	10 (76.9)	0.99[c]
M1	1 (2.5)	1 (3.7)	0 (0)	
NA	8 (20.0)	5 (18.5)	3 (23.1)	
Resection margins, n (%)				
R0	37 (92.5)	26 (96.3)	11 (84.6)	0.24[c]
R1	1 (2.5)	0 (0)	1 (7.7)	
NA	2 (5.0)	1 (3.7)	1 (7.7)	
Histological grade, n (%)				
G1	0 (0)	0 (0)	0 (0)	0.99[c]
G2	17 (42.5)	12 (44.5)	5 (38.5)	
G3	15 (37.5)	10 (37.0)	5 (38.5)	
NA	8 (20.0)	5 (18.5)	3 (23.0)	
Tumour size at surgery (cm) median (range)	6 (2–18)	6 (2–9)	7 (4–18)	0.16[a]

hENT-1, human equilibrative nucleoside transporter 1; iCC, intrahepatic cholangiocarcinoma.
[a] Mann–Whitney U test.
[b] Pearson's chi-square test.
[c] Fisher's exact test.

median value. Tests based on the Schoenfeld residuals along with graphical methods were used to detect violations of the proportional hazard assumption [12]. To evaluate the predictive power of a model, Harrell's C index and corresponding 95% CI were calculated (using the package for STATA 14.2) [13,14].

To minimise the effect of potential confounders on selection bias, a propensity score was derived reflecting the probability of a patient expressing membrane hENT-1, given a set of possible confounders [15,16]. To accomplish this, we first constructed a multivariable logistic regression model using hENT-1 localisation in tumour cells as a dependent variable and entering patient's covariates in the model. These variables included age (categorised by tertiles), gender, disease stage, histological grade and tumour size at surgery (entered as binary). Then, we fitted Cox proportional hazards regression models adjusted by propensity score included either as linear term or stratified on quintiles. For *in vitro* assays, differences between groups were analysed using Student *t* test. Cohen's k was used for interobserver agreement in the hENT-1 IHC evaluation. Statistical analyses were performed using Stata 14.2 SE (Stata Corporation, College Station, TX, USA). All the tests were two-sided, and a p value < 0.05 was defined as statistically significant.

3. Results

3.1. Patient characteristics

Of the 48 consecutive iCC patients considered fit for adjuvant gemcitabine but who did not receive treatment because they declined, eight were excluded from the study due to the lack of follow-up. Finally, 40 iCC patients were retrospectively included in the study; the main clinical-pathological variables are summarised in Table 1. The cohort consisted of 19 men and 21 women with a median age at diagnosis of 63.5 years (range, 34–77). Median tumour size was 6 cm (range 2–18 cm). Tumours were grade I in 0 (0%) cases, grade II in 20 (50%) cases and grade III in 20 (50) cases. Five patients (12.5%) were classified as T1, 24 (60%) as T2 and 11 (27.5%) as T3. All iCCs were mass-forming type with associated areas of periductal infiltrating growth in two (5.0%) cases. Microvascular and/or perineural neoplastic invasion was present in 31 (77.5%) cases. Thirty-three (82.5%) iCCs arose on non-cirrhotic livers, two (5.0%) in livers with fibrous septa and five (12.5%) in cirrhotic livers. Twelve (30.0%%) patients had locoregional lymph node metastasis.

3.2. hENT-1 protein is expressed in iCC but not in matched non-tumoural liver tissues

Few data have been reported on hENT-1 expression in iCC and matched non-tumoural liver tissue. To better clarify this issue, we first evaluated hENT-1 mRNA expression in the tumour and matched non-tumoural liver counterpart from the 40 iCC patients included in the study. We observed that hENT-1 mRNA expression was significantly higher in tumours than in matched non-tumoural liver tissues (Fig. 1A). To further validate these findings, hENT-1 protein level was determined by Western blot analysis. Twenty-eight (70%) of the 40 iCCs were found to express hENT-1 protein, whereas 12

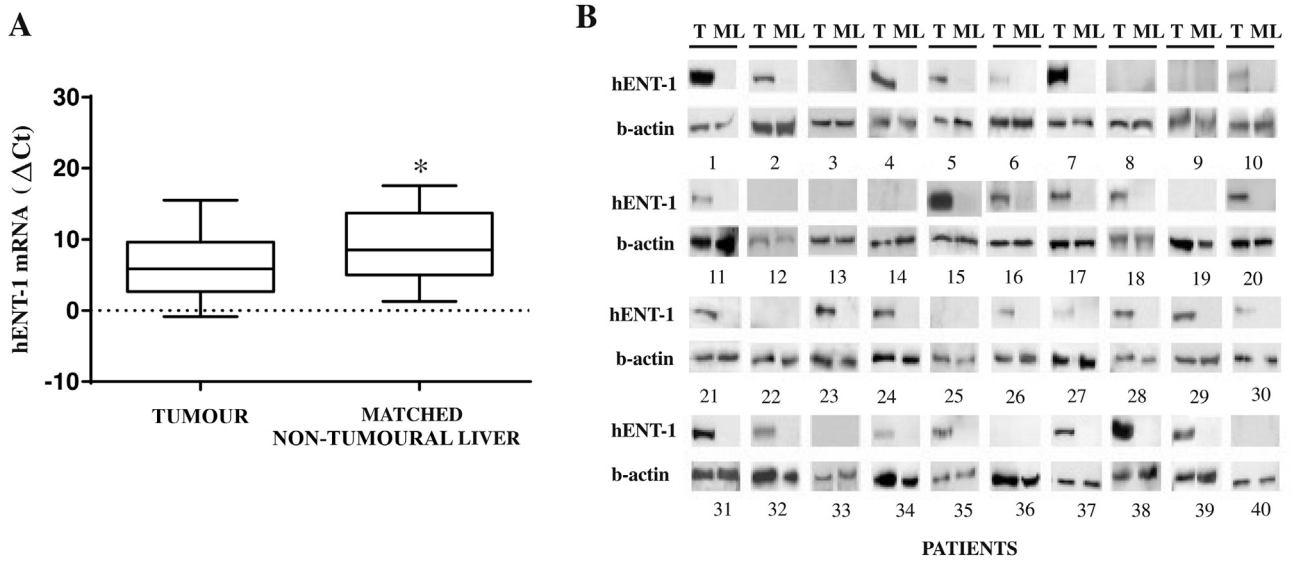

Fig. 1. A) Box-plot analysis of hENT-1 mRNA expression in 40 iCC tumour tissues and matched non-tumoural livers. Results are expressed as ΔCt (Ct of hENT-1 gene normalised to Ct of GADPH gene). A lower ΔCt value refers to a higher hENT-1 mRNA expression. *$p < 0.05$; (B) Western blot analysis of hENT-1 protein expression in 40 iCC tumour tissues and the matched non-tumoural liver. β-actin was assessed as a quantitative control for equal loading. T, tumour tissue; ML, matched non-tumoural liver; hENT-1, human equilibrative nucleoside transporter 1; iCC, intrahepatic cholangiocarcinoma.

(30%) tumour samples were negative (Fig. 1B). Notably, all matched non-tumoural livers were negative for hENT-1 protein expression (Fig. 1B). These findings were in line with IHC results (Fig. 2). Indeed, IHC analysis of the matched non-tumoural liver revealed that hENT-1 was not expressed by either normal cholangiocytes or hepatocytes (Fig. 2a–c).

3.3. Membrane hENT-1 is associated with higher Ki67 proliferation index in iCC tissues

In the light of the physiological role of hENT-1 as a membrane transporter of nucleosides for NTP synthesis, we next investigated the possible association between hENT-1 cellular localisation and the proliferation marker Ki67. The interobserver agreement among the three pathologists in hENT-1 evaluation was good ($k = 0.83$); the discordant cases were collegially discussed. IHC on TMA revealed that 12 (30%) cases were completely negative for hENT-1 expression in tumour tissue, 15 (37.5%) displayed only a cytoplasmic staining, whereas 13 (32.5%) showed a concomitant cytoplasmic/membrane hENT-1 positivity (Fig. 3A).

Eighteen (45%) of 40 cases showed a Ki67 nuclear staining ≥10%, whereas in 22 of 40 cases (55%), it was <10% (Fig. 3A). Membrane hENT-1–positive patients were found to have a higher percentage of Ki67-positive cells in tumour tissue (median 23%, range 13–63%) than membrane hENT-1–negative patients (median 5%, range 0–15%) ($p < 0.0001$) (Fig. 3B). In particular, only five membrane hENT-1–negative patients (18%) had Ki67-positive cells ≥ 10%, whereas all 13 membrane hENT-1–positive patients (100%) had Ki67-positive cells ≥ 10% ($p < 0.0001$) (Table 2). In addition, survival analysis revealed that membrane hENT-1–positive patients had a shorter OS (median 21.2 months, range 3.5–52.5) than membrane hENT-1–negative patients (median 30.3 months, range 5.6–67) (Fig. 3C). Estimates for the association between membrane hENT-1 localisation and OS are reported in Table 3. Unadjusted

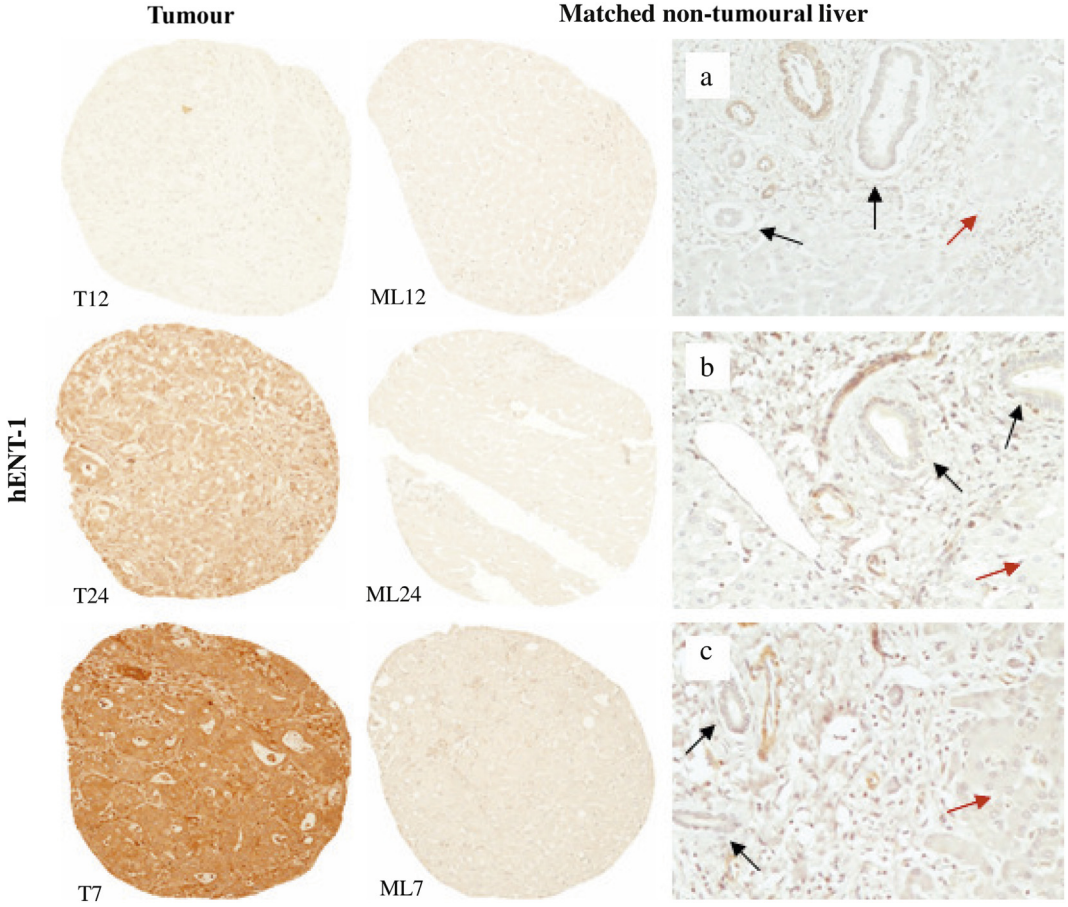

Fig. 2. Three representative cases of iCC on TMA showing different hENT-1 immunostaining (left column, 20× magnification): T12 is completely negative for the transporter; T24 shows a moderate positivity and T7 shows a high immunoreactivity. For each case, hENT-1 immunoreaction in matched non-tumoural liver is also reported (middle column, 20× magnification). Matched non-tumoural livers at higher magnification (40×) show normal bile ducts (black arrows) and hepatocytes (red arrows) completely negative for hENT-1 expression (right column). T, tumour tissue; ML, matched non-tumoural liver; hENT-1, human equilibrative nucleoside transporter 1; iCC, intrahepatic cholangiocarcinoma; TMA, tissue microarray.

estimates were close to those produced with the multivariable Cox regression analysis. The multivariable model had good discrimination (Harrel's C index 0.71, 95%CI 0.58–0.84). The estimates adjusted via propensity score were consistent with those obtained by the multivariable model alone. Membrane-positive hENT-1 was associated with shorter OS (adjusted HR by propensity score (linear term) 2.61, 95% CI 1.00–6.82; adjusted HR by propensity score (quintiles) 2.87, 95% CI 1.03–7.98) than membrane-negative hENT-1.

To further confirm the positive association between membrane hENT-1 and high Ki67 score, IHC analysis

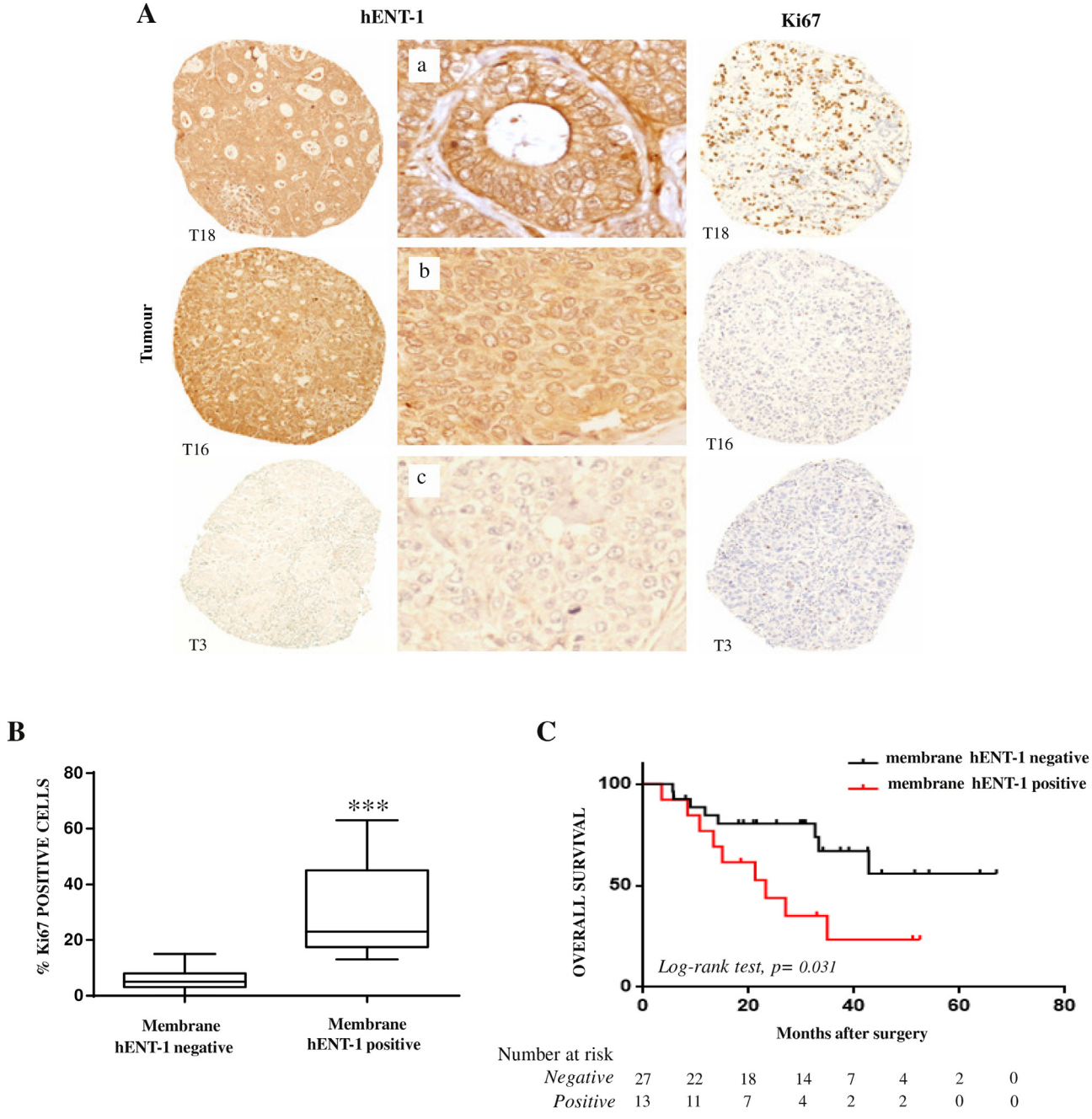

Fig. 3. A) Three representative cases of iCC on TMA showing the correlation between hENT-1 cellular localisation (left and middle columns) and Ki67 immunohistochemical expression (right column). T18 (first row) shows a high Ki67 immunoreactivity and hENT-1 clearly localised on both tumour cell membrane and cytoplasm. T16 (second row) shows a very low Ki67 immunostaining, and albeit showing a hENT-1 immunostaining similar to T18 at 20× magnification, the transporter is localised only in the cytoplasm of tumour cells. Finally, T3 (third row) displays a very low Ki67 immunostaining and a total negativity for hENT-1 expression in tumour cells. Left and right columns: magnification 20×; middle column: magnification 40×; (B) box-plot analysis of Ki67-positive cells in 40 iCC samples based on membrane hENT-1 localisation. ***$p < 0.0001$; (C) overall-survival curves of 40 iCC patients stratified based on membrane hENT-1 localisation ($p = 0.031$). T, tumour tissue; hENT-1, human equilibrative nucleoside transporter 1; iCC, intrahepatic cholangiocarcinoma.

was performed in the independent cohort of 44 iCC patients belonging to our previous study [6]. Of these, 25 (57%) of the 44 cases showed a Ki67 nuclear staining ≥10%, whereas 19 (43%) had <10% (Supplementary Fig. 1A). Membrane hENT-1–positive patients resulted in a higher percentage of Ki67-positive cells in tumour tissue (median 17.5%, range 9–45%) than membrane hENT-1–negative patients (median 8%, range 5–30%) ($p < 0.0001$) (Supplementary Fig. 1B). Notably, in the subgroup of membrane hENT-1–negative patients, 10 (35.7%) of 28 cases had Ki67-positive cells ≥ 10%, whereas among membrane hENT-1–positive patients, 15 (93.7%) of 16 cases had Ki67-positive cells ≥ 10% ($p = 0.0002$) (Supplementary Table 1).

Overall, these findings strongly support the notion that membrane hENT-1 characterises iCCs with a high proliferation rate.

3.4. Membrane hENT-1 regulates cell growth and survival in iCC cell lines

To better clarify the involvement of membrane hENT-1 localisation in regulating iCC tumour growth, we evaluated the expression/localisation of the transporter in two iCC cell lines, HuH-28 and SNU-1079. Immunocytochemistry and Western blot analysis of both cytosolic and membrane fractions revealed that SNU-1079 cells expressed hENT-1 only in the cytoplasm, whereas HuH-28 cells expressed the transporter both in the cytoplasm and on the cell membrane (Fig. 4A and B). Next, cell lines were transfected with hENT-1 siRNA. We observed a significant decrease in mRNA and protein expression in HuH-28 and SNU-1079 cells after 72 and 48 h of incubation, respectively (Fig. 4C). Notably, hENT-1 silencing was associated with a significant decrease of HuH-28 cell growth at 72 h compared with scramble cells. Conversely, no significant change in cell growth was observed in SNU-1079 cells either at 48 or 72 h of hENT-1 silencing (Fig. 5A and B and Supplementary Fig. 2A and B). Cell cycle analysis showed that hENT-1 silencing in HuH-28 cells resulted in an accumulation in G0-G1 and sub-G0 phase, with a corresponding decrease of G2/M and S phase fractions, compared with scramble cells (Fig. 5C). Conversely, no significant differences in cell cycle phases were found between hENT-1 silenced and scramble SNU-1079 cells (Fig. 5D). Further western blot analysis revealed that the increase in sub-G0 phase in HuH-28 silenced cells was related to apoptosis induction, as shown by caspase-3/PARP-1 cleavage in this cell line, but not in SNU-1079 cells (Fig. 5E and F, upper panel). These results were in line with Hoechst staining that revealed the presence of typical apoptotic figures only in HuH-28 silenced cells (Fig. 5E and F, lower panel).

Overall these findings suggest that membrane hENT-1 localisation is involved in the regulation of iCC cell growth and survival.

4. Discussion

Most iCCs are characterised by an aggressive biological behaviour and show rapid tumour growth; however the molecular mechanisms underlying this phenomenon have yet to be fully elucidated. The present study explored the possible involvement of the nucleoside transporter hENT-1 in regulating iCC tumour growth and predicting the survival of resected iCC patients not receiving adjuvant treatments. We observed that hENT-1 mRNA was expressed both in iCC and matched non-tumoural liver tissues, even if at lower levels. Conversely, hENT-1 protein was expressed only in iCC samples, suggesting a posttranscriptional regulation in non-tumoural liver. These findings are in line with previous studies reporting a higher expression of hENT-1 in proliferating cells than non-cycling growth-arrested cells [17]. Indeed, in normal conditions the liver is a silent organ, with a very slow turnover of both hepatocytes and cholangiocytes. Conversely, iCC is characterised by a high cell turnover and proliferation activity, a condition requiring a considerable amount of nucleosides for NTP synthesis (essential to sustain DNA replication and RNA production during cell division) and that may justify the increased expression of hENT-1 in this tissue type. However, because an efficient intracellular uptake of nucleosides requires hENT-1 to be localised on the cell membrane [18,19], here, we hypothesised that an aberrant localisation of this transporter in tumour cells may result in impaired nucleoside uptake, thereby affecting the intracellular NTP pool and finally iCC tumour growth. In line with this hypothesis, a positive correlation between membrane hENT-1 and a high Ki67 score was found in our iCC cases. Conversely, iCCs expressing the transporter only in the cytoplasm were associated with a low Ki67 staining, similar to that observed in iCCs negative for hENT-1 expression. Notably, these findings were also confirmed in the independent cohort of 44 iCC patients belonging to our previous study [6]. Moreover, patients harbouring membrane hENT-1 in iCC tissue were found to have a shorter OS than membrane hENT-1–negative patients, suggesting that hENT-1 tumour localisation could serve as a potential prognostic factor in this malignancy.

Table 2
Correlation between hENT-1 membrane localisation and Ki67 labelling index in the 40 iCC patients included in the study.

hENT-1 Membrane status	Ki67 ≥ 10%	Ki67 < 10%	p-value[a]
Membrane hENT-1 negative	5 (18%)	22 (82%)	<0.0001
Membrane hENT-1 positive	13 (100%)	0 (0%)	

hENT-1, human equilibrative nucleoside transporter 1; iCC, intrahepatic cholangiocarcinoma.
For Ki67, a cut-off of ≥10% and <10% nuclear staining was chosen to discriminate between high and low expression, respectively.
[a] Chi-square test.

Table 3
Hazard ratios (HRs) and corresponding 95% confidence intervals (CI) among the 40 patients who had undergone surgical resection for iCC based on hENT-1 localisation in tumour cells.

Membrane hENT-1 status	Crude model		Multivariable model[a]		PS-adjusted (linear term) model[b]		PS-adjusted (quintiles) model[c]	
	HR	95%CI	HR	95%CI	HR	95%CI	HR	95%CI
Negative	1.00	Ref.	1.00	Ref.	1.00	Ref.	1.00	Ref.
Positive	2.74	1.05–7.13	2.80	1.01–7.76	2.61	1.00–6.82	2.87	1.03–7.98

hENT-1, human equilibrative nucleoside transporter 1; iCC, intrahepatic cholangiocarcinoma; PS, propensity score.
[a] Estimates from Cox proportional hazards regression model adjusted for selected covariates (age [entered as categorical variable], gender, disease stage, histological grade and tumour size [entered as binary variable]).
[b] Estimates from Cox proportional hazards regression model adjusted for PS (linear term).
[c] Estimates from Cox proportional hazards regression model adjusted for PS (quintiles).

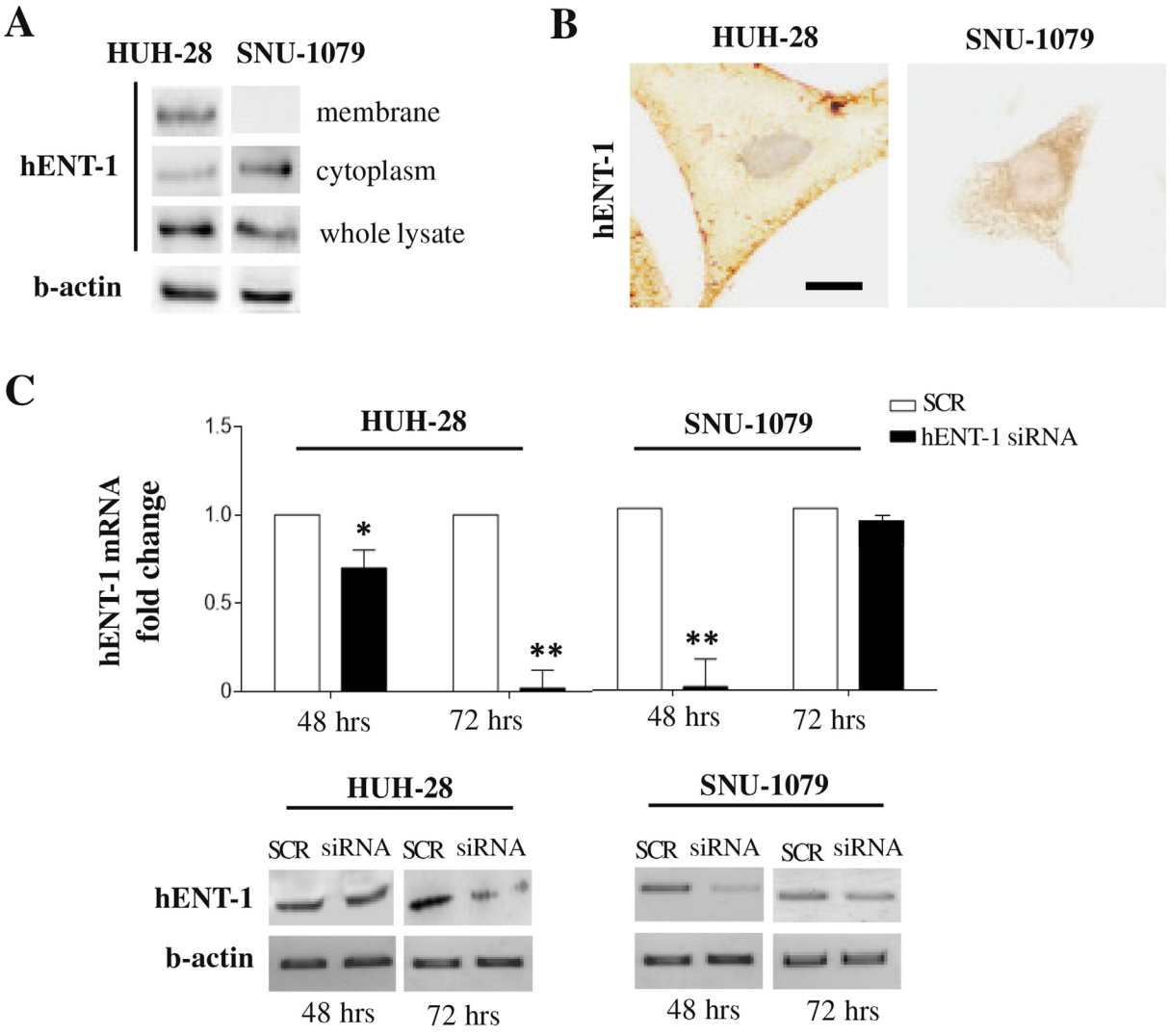

Fig. 4. A) Western blotting analysis of hENT-1 protein expression in membrane, cytoplasmic and whole cell lysate of HuH-28 and SNU-1079 cell lines. β-actin was assessed as a quantitative control for equal loading; (B) immunocytochemistry analysis of hENT-1 intracellular localisation in HuH-28 and SNU-1079 iCC cell lines. Scale bar: 10 μm; (C) (Upper panel) hENT-1 mRNA fold change in HuH-28 and SNU-1079 cell lines transfected with hENT-1 siRNA and scramble (SCR) for 48 and 72 h. *$p < 0.05$; ** $p < 0.001$; (Lower panel) western blotting analysis of hENT-1 protein expression in HuH-28 and SNU-1079 cell lines transfected with hENT-1 siRNA and SCR for 48 and 72 h. β-actin was assessed as quantitative control for equal loading. hENT-1, human equilibrative nucleoside transporter 1; iCC, intrahepatic cholangiocarcinoma.

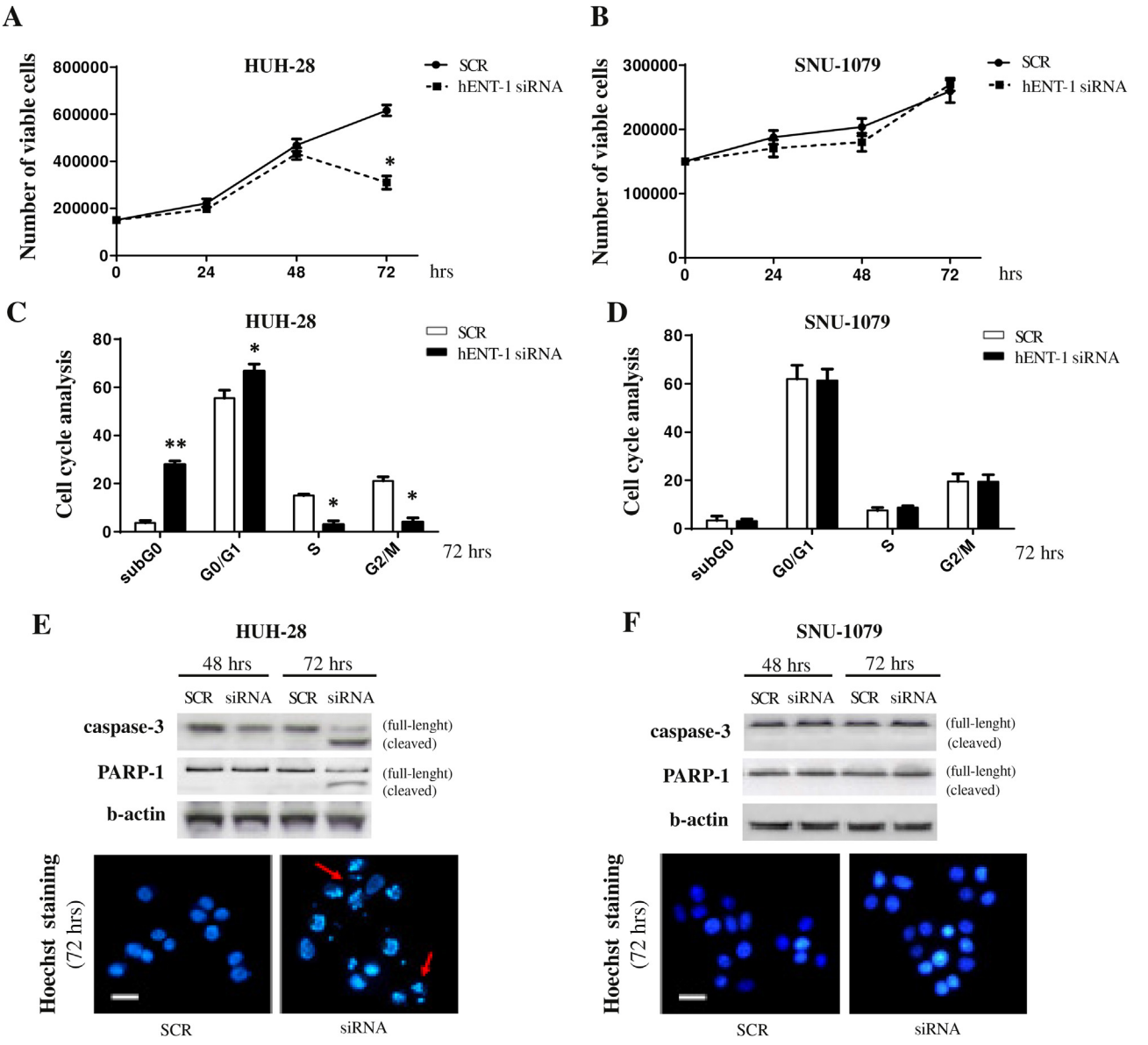

Fig. 5. A), (B) MTT assay in HuH-28 and SNU-1079 iCC cell lines transfected with hENT-1 siRNA and scramble (SCR) for 24, 48 and 72 h. *$p < 0.05$; (C), (D) cell cycle analysis in HuH-28 and SNU-1079 iCC cell lines transfected with hENT-1 siRNA and SCR for 72 h. *$p < 0.05$, **$p < 0.001$; (E, F) (Upper panel) Western blotting analysis of full-length/cleaved caspase-3 and PARP-1 in HuH-28 and SNU-1079 cell lines transfected with hENT-1 siRNA and SCR for 48 and 72 h. β-actin was assessed as a quantitative control for equal loading. (Lower panel) Fluorescence microscopy analysis of HuH-28 and SNU-1079 cells transfected with hENT-1 siRNA and SCR for 72 h and stained with 1 mg/ml Hoechst 33,342. Red arrows show the typical nuclear morphology of cells undergoing apoptosis. Scale bar: 20 μm. hENT-1, human equilibrative nucleoside transporter 1; iCC, intrahepatic cholangiocarcinoma; MTT, methyltetrazolium; PARP, poly-(ADP-ribose) polymerase-1.

A high hENT-1 protein expression has been already reported to associate with shorter OS and high Ki67 score in ampullary carcinoma [20]. Even if the association between Ki67 staining and hENT-1 localisation has not been investigated in this previous study, it is conceivable that, similarly to our iCC cases (where membrane hENT-1 positivity invariably occurred together with a cytoplasmic positivity), some of the ampullary carcinomas with high hENT-1 cytoplasmic staining also had a concomitant membrane hENT-1 staining, not detectable because of important variables in IHC analysis (such as time of tissue fixation, type of fixation, long-term stability of the epitope and the specificity of the antibody used).

To better clarify the role of hENT-1 localisation in the regulation of iCC cell growth, functional analyses in iCC cell lines were performed. Previous studies have reported that an insufficient NTP supply within cells may result in dysfunctional proliferation, DNA damage and finally apoptosis [21]. Moreover, reduced expression

of the isoform hENT-2 has been shown to result in a dramatic decrease in cell proliferation and dysregulation of the cell cycle, due to a lower incorporation of NTPs into DNA [22]. In line with these observations, hENT-1 silencing was found to inhibit cell proliferation and induce apoptosis in HUH-28 cells, expressing hENT-1 on the cell membrane. Conversely, no significant changes in these parameters were observed in silenced SNU-1079 cells expressing hENT-1 only in the cytoplasm. This last result is not totally surprising; indeed, although the uptake of nucleosides mostly occurs *via* hENT-1, other transporters (including hENT-2) may be involved in this process, even if to a lesser extent [22]. Therefore, failure of apoptosis induction in hENT-1–silenced SNU-1079 cells could be related to the maintenance of a proper intracellular NTP pool by nucleoside transporters other than hENT-1.

In conclusion, the present study suggests that membrane hENT-1 characterises iCCs with a high proliferation rate and is associated with worse OS in resected patients not receiving adjuvant treatments. In the light of our previous study in the adjuvant setting [6], overall, our findings support the notion that, similarly to human epidermal growth factor receptor 2 (HER2)/neu in breast cancer (where its overexpression associates with worse survival, but with response to anti-HER2 therapies [23]), membrane hENT-1 may represent a worse prognostic factor, but a predictive factor of efficacy of gemcitabine-based chemotherapy, in iCC.

However, due to the retrospective nature of the present study and the limited number of included cases, further prospective studies on larger cohorts of iCC patients are required to confirm these results.

Conflict of interest statement

None declared.

Acknowledgements

This work was supported by Fondazione Cassa di Risparmio di Bologna (Italy, grant ID:2014/0231) to Prof. G. Brandi.

Appendix A. Supplementary data

Supplementary data to this article can be found online at https://doi.org/10.1016/j.ejca.2018.11.005.

References

[1] Buettner S, van Vugt JL, IJzermans JN, et al. Intrahepatic cholangiocarcinoma: current perspectives. OncoTargets Ther 2017;10:1131–42.
[2] Razumilava N, Gores GJ. Cholangiocarcinoma. Lancet 2014;383:2168–79.
[3] Ribero D, Pinna AD, Guglielmi A, et al., Italian Intrahepatic Cholangiocarcinoma Study Group. Surgical approach for long-term survival of patients with intrahepatic cholangiocarcinoma: a multi-institutional analysis of 434 patients. Arch Surg 2012;147:1107–13.
[4] Mao Z, Guo X, Su D, et al. Prognostic factors of cholangiocarcinoma after surgical resection: a retrospective study of 293 patients. Med Sci Monit 2015;21:2375–81.
[5] Huang W, Zeng X, Shi Y, et al. Functional characterization of human equilibrative nucleoside transporter 1. Protein Cell 2017;8:284–95.
[6] Brandi G, Deserti M, Vasuri F, et al. Membrane localization of human equilibrative nucleoside transporter 1 in tumor cells may predict response to adjuvant gemcitabine in resected cholangiocarcinoma patients. Oncologist 2016;21:600–7.
[7] Di Girolamo S, Nobili E, Derenzini E, et al. Impact of adjuvant chemotherapy on time to relapse in cholangiocarcinoma. In: Gastrointestinal cancers symposium. Journal of Clinical Oncology, vol. Suppl. 4, Vol. 29, p. xx, ISSN: 0732-183X, San Francisco (CA), 19-21 January 2011; 2011.
[8] Bosman FT, Carneiro F, Hruban RH, et al. WHO/IARC Classification of tumors of the digestive system. 4th ed. 2010. Lyon.
[9] American Joint Committee on Cancer (AJCC). Cancer staging manual. 8th ed. New York: Springer; 2017.
[10] Brandi G, Farioli A, Astolfi A, et al. Genetic heterogeneity in cholangiocarcinoma: a major challenge for targeted therapies. Oncotarget 2015;6:14744–53.
[11] Greenland S, Daniel R, Pearce N. Outcome modelling strategies in epidemiology: traditional methods and basic alternatives. Int J Epidemiol 2016;45:565–75.
[12] Grambsch PM, Therneau TM. Proportional hazards tests and diagnostics based on weighted residuals. Biometrika 1994;81:515–26.
[13] Newson RB. Confidence intervals for rank statistics: Somers' D and extensions. Stata J 2006;6(3):309–34.
[14] Newson RB. Comparing the predictive powers of survival models using Harrell's C or Somers' D. Stata J 2010;10(3):339–58.
[15] Rosenbaum PR, Rubin DB. The central role of the propensity score in observational studies for causal effects. Biometrika 1983;70:41–55.
[16] D'Agostino Jr RB. Propensity scores in cardiovascular research. Circulation 2007;115(17):2340–3.
[17] Plotnik DA, Asher C, Chu SK, et al. Levels of human equilibrative nucleoside transporter-1 are higher in proliferating regions of A549 tumor cells grown as tumor xenografts in vivo. Nucl Med Biol 2012;39:1161–6.
[18] Endo Y, Obata T, Murata D, et al. Cellular localization and functional characterization of the equilibrative nucleoside transporters of antitumor nucleosides. Cancer Sci 2007;98:1633–7.
[19] Nivillac NM, Wasal K, Villani DF, et al. Disrupted plasma membrane localization and loss of function reveal regions of human equilibrative nucleoside transporter 1 involved in structural integrity and activity. Biochim Biophys Acta 2009;1788:2326–34.
[20] Santini D, Perrone G, Vincenzi B, et al. Human equilibrative nucleoside transporter 1 (hENT1) protein is associated with short survival in resected ampullary cancer. Ann Oncol 2008;19:724–8.
[21] Oliver FJ, Collins MK, López-Rivas A. dNTP pools imbalance as a signal to initiate apoptosis. Experientia 1996;52:995–1000.
[22] Grañé-Boladeras N, Spring CM, Hanna WJ, et al. Novel nuclear hENT2 isoforms regulate cell cycle progression via controlling nucleoside transport and nuclear reservoir. Cell Mol Life Sci 2016;73:4559–75.
[23] Nicolini A, Ferrari P, Duffy MJ. Prognostic and predictive biomarkers in breast cancer: past, present and future. Semin Cancer Biol 2018;52:56–73.